

# Progress in Lattice QCD at nonzero density using the Complex Langevin equation

Dénes Sexty

Bergische Universität Wuppertal

E-mail: [sexty@uni-wuppertal.de](mailto:sexty@uni-wuppertal.de)

**Abstract.** Recent progress in direct simulations of QCD at nonzero chemical potentials is reported upon. After a brief introduction to the sign problem in lattice QCD and a quick description of the complex Langevin equation we show recent results and discuss open questions.

## 1. Introduction

Lattice simulations of QCD are based on a path integral formulation using the partition sum

$$Z = \int DU e^{-S_g[U]} \det M(\mu, U), \quad (1)$$

with the gauge action of the link variables  $S_g[U]$ , and the fermion matrix  $M(\mu, U)$ , where the dependence on the quark chemical potential  $\mu$  is indicated. At  $\mu = 0$  the measure in this integral is positive, therefore importance sampling can be used to calculate various thermodynamical operators, propagators, etc. In contrast, at  $\mu \neq 0$  the determinant is in general complex resulting in a *Sign problem*, invalidating direct simulations with importance sampling. Many methods have been proposed to evade the sign problem, see the reviews in the context of lattice QCD [1]. Most of these methods have some shortcomings, typically they are applicable at low chemical potentials ( $\mu < T$  with the temperature  $T$ ). While there are many proposals for different dense phases as well as a critical point, a large part of the phase diagram of QCD still remains unknown.

Recently two methods using analyticity have emerged as good candidates for an eventual solution of the QCD sign problem. They are the Complex Langevin equation (CLE)[2] and the Lefschetz thimble method [3]. Both are based on the complexification of the field manifolds, with the CLE expanding the theory to this manifold, while the thimble method shifting the original manifold into the complex plane while keeping the dimension of integrations fixed.

The Complex Langevin method was invented more than thirty years ago as a generalization of the stochastic quantization [4] (which uses the real Langevin equation), but it has had many practical problems over the years as well as unsatisfactory theoretical understanding. Recently there has been a definite progress in both grounds: On the theoretical side, there is a theorem which guarantees correct results as long as some conditions are satisfied [5]. Coupled with the gauge cooling procedure [6] this has allowed direct simulations of among others full QCD with light quarks [7, 8], at least in the high temperature regime.

The CLE is briefly introduced in section 2 and some results are presented in section 3.



## 2. The complex Langevin equation

The complex Langevin equation for scalar field  $x$  and action  $S(x)$  is written as

$$\partial_\tau x = -\partial_x S(x) + \eta(\tau) \quad (2)$$

with the Gaussian noise  $\eta(\tau)$  satisfying  $\langle \eta(\tau)\eta(\tau') \rangle = \delta(\tau - \tau')$ . For a complex action the fields are complexified, and the original theory is supposed to be recovered by analytical continuation

$$\int dx P(x) O(x) = \int dx dy P(x, y) O(x + iy) \quad (3)$$

where  $P(x) = \exp(-S(x))$  is the (complex) measure on the real axis,  $P(x, y)$  is the real probability distribution of the complexified scalar field constructed by solving the complex Langevin equation. In practice this means that one calculates the average by collecting data along the solution of the CLE for the analytically continued observables (after thermalization). For holomorphic actions the correctness of the results can be assessed by observing the decay of  $P(x, y)$  at large  $x$  and  $y$  [5], where wrong convergence is signalled by slow (power law) decay.

For gauge theories the discretised update is written as

$$U_{x,\nu}(\tau + \epsilon) = \exp \left[ i \sum_a \lambda_a (-\epsilon D_{ax\nu} S[U] + \sqrt{\epsilon} \eta_{ax\nu}) \right] U_{x,\nu}(\tau), \quad (4)$$

where  $\lambda_a$  are the generators of the gauge group, i.e. the Gell-Mann matrices. The drift force is calculated from the action  $S[U]$  with the left derivative

$$D_{ax\nu} f(U) = \partial_\alpha f(e^{i\alpha \lambda_a} U_{x,\nu}) \Big|_{\alpha=0}. \quad (5)$$

Here a complex action leads to a complex drift force, and thus the original  $SU(3)$  manifold of the link variables expands to the non-compact  $SL(3, \mathbb{C})$ , i.e. they are no longer unitary. Since the gauge symmetry also complexifies, each configuration has a gauge orbit with infinite volume. In practice this leads to the breakdown of naive CLE simulations of gauge theories. This behaviour is cured by gauge cooling [6], which uses the imaginary directions of the gauge symmetry to get the configurations closer to the original manifold, and thus keeping the system from trying to explore the non-compact directions of  $SL(3, \mathbb{C})$  connected to gauge symmetry.

In the case of fermionic theories, an additional problem can appear, as the measure of the theory is written as  $e^{-S_g[U]} \det M(U, \mu)$ . This measure can have zeroes on the complexified manifold, which is reflected by a pole in the drift term. If the distribution around the singularities is non-vanishing, incorrect results can be obtained, as first noticed in [9]. A zero of the measure outside the support of the complexified distribution can not invalidate the results, but in contrast, it can lead to incorrect results even in the cases where fast decay is observed, if the process gets close to the singularities [10]. Recently it has been proposed that a variation of the gauge cooling algorithm might be able to modify the process such that the zeros of the measure are avoided [11].

## 3. Numerical Results

Heavy dense QCD (HDQCD) is defined by dropping the spatial fermionic hoppings from  $M(U, \mu)$ , which thus corresponds to static fermionic particles. This can also be understood as the simultaneous limit  $m, \mu \rightarrow \infty$  with the bare quark mass  $m$ , while the combination  $\kappa e^\mu$  is kept fixed with  $\kappa = 1/(4m)$ . HDQCD shares common features with QCD, while it is much simpler, in particular the fermionic determinant simplifies to a product of spatially local determinants. It has been studied with the CLE [6] as well as reweighting [12]. In the CLE

treatment the gauge cooling stabilizes simulations as long as the lattice spacing is not too large (corresponding to a lower limit of the  $\beta$  parameter of the plaquette action). This allows to map out the phase diagram by fixing  $\beta$  to some fixed value, and changing the temporal extent of the lattice to perform a temperature scan. The chemical potential can be freely changed, the CLE method works fine also in the cases where the sign problem is hard. The Polyakov loop and the fermionic density is plotted in Fig. 1. The onset transition at high chemical potentials is nicely indicated by the fermionic density. One also observes that the transition gets sharper at lower densities, as required by the Silver-Blaze phenomenon. At higher chemical potentials, the fermionic density saturates, as all the available fermionic states on the lattice are filled. The deconfinement transition at zero chemical potential is shown by the nonzero value of the Polyakov loop, as well as the onset transition at high chemical potentials. The decay at large chemical potential is the consequence of the lattice artifact of saturation, therefore it has no relevance for continuum physics. So in this theory the onset transition and the deconfinement seem to be connected. The order of the transitions can be determined with e. g. finite size scaling [13]. The phase diagram of HDQCD is thus very simple compared to the expected phase diagram of full QCD, this is because quarks can't move spatially in this theory.

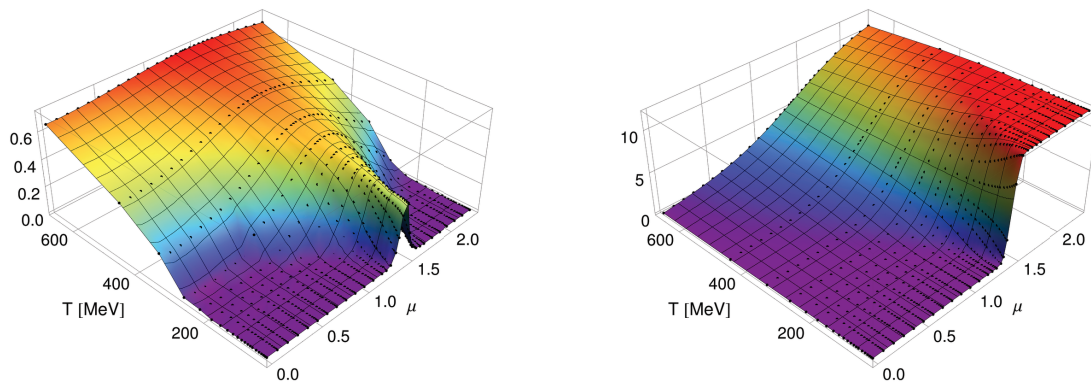


**Figure 1.** The Polyakov loop(left) and the fermionic density(right) as a function of the temperature and the chemical potential (in lattice units) in HDQCD at  $\beta = 5.8$  and  $\kappa = 0.12$ .

In full QCD the fermionic contribution to the drift term is written as

$$K_{ax\nu}^F = \frac{N_F}{4} \text{Tr}[M^{-1}(\mu, U) D_{ax\nu} M(\mu, U)]. \quad (6)$$

As this involves the inverse of the typically very large matrix  $M(\mu, U)$ , a stochastic estimator is used to calculate it using the Conjugate Gradient (CG) algorithm [7]. Here we report on simulations using the plaquette action and unimproved staggered fermions. Using gauge cooling this procedure allows simulations at not too small  $\beta$  values. The main cost of the simulations is the inversion of fermionic matrix with CG, similarly to Hybrid Monte Carlo (HMC) simulations. In Fig. 2 the behavior of various observables as a function of the chemical potential is shown at some fixed temperature in the deconfined phase. One observes the expected behavior with the increase and eventual saturation of the fermionic density, also signalled by the Polyakov loops and its inverse as well as the chiral condensate.

We have performed comparisons between the CLE and the multiparameter reweighting method [14], where one rewrites the measure using a positive ensemble e.g. using zero chemical potential [15]. This allows to use HMC simulations, however overlap and sign problems might

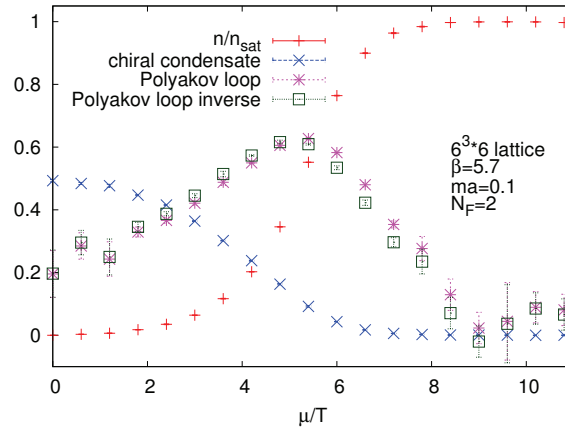


**Figure 2.** Various observables measured in full QCD with 2 flavours of staggered fermions as a function the chemical potential at a fixed temperature. The quantities are plotted in lattice units.

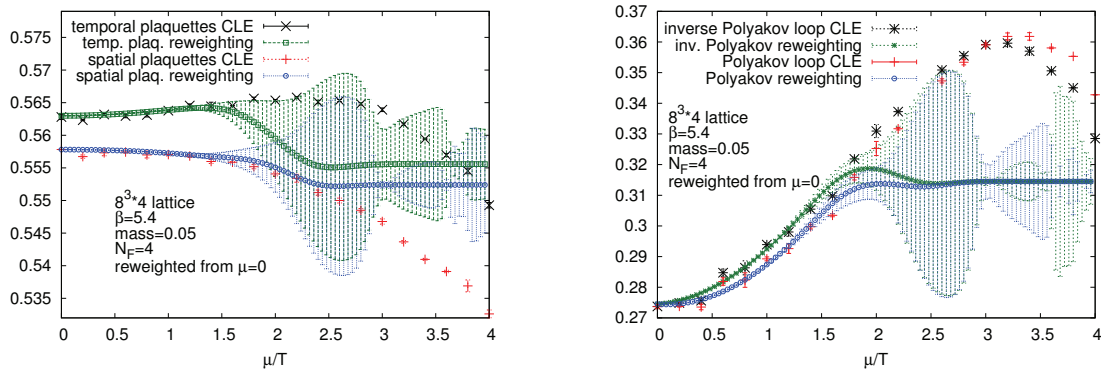


**Figure 3.** The spatial plaquettes (left) and the Polyakov loop (right) measured using the CLE and reweighting as a function of the chemical potential.

prevent extracting usable results if  $\mu$  is large. In Fig. 3 we show the spatial plaquettes and the Polyakov loop at a fixed temperature in the deconfined phase as a function of the chemical potential. One notes that the reweighting starts to develop large errors around  $\mu = 1.5T$  signalling unreliable results, while the complex Langevin results follow the expected behavior. The correctness of CLE can also be independently assessed by looking at distributions of observables, where a slow (power law) decay indicates wrong results.

In Fig. 4 the Polyakov loop is shown as a function of the  $\beta$  parameter of the action. We have increased the lattice size to  $N_T = 6$  and 8 while keeping the pion mass over the temperature approximately fixed, and also exploring a system with larger pion mass at  $N_T = 8$ . As expected, at low  $\beta$ , the CLE simulations break down, similarly to HDQCD, as the gauge cooling can not keep the process close to the SU(3) manifold. In HDQCD, increasing the lattice size allowed to go into the confined phase already at  $N_T = 8$ . In contrast, full-QCD results show that  $N_T = 8$  is not sufficient to reach into the confined phase. It is an open question whether a further increase in the lattice size alone will allow for exploration of the confined phase in full QCD.

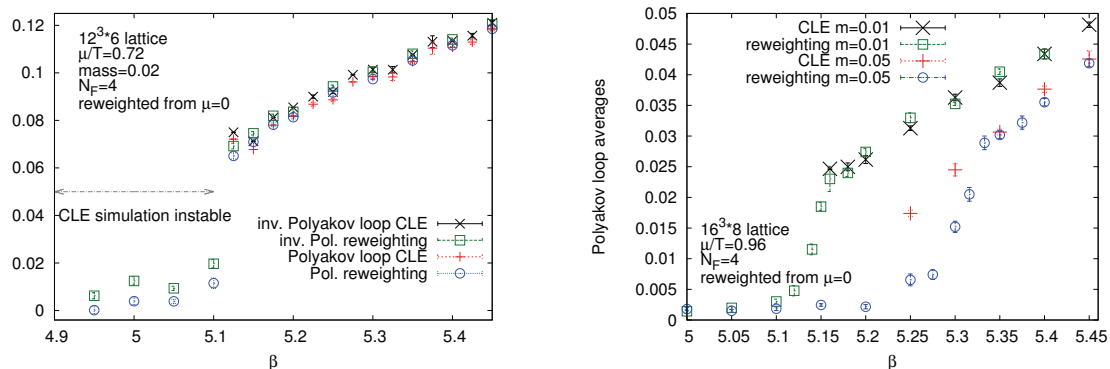


**Figure 4.** The Polyakov loop on  $12^3 \times 6$  (left) and  $16^3 \times 8$  (right) lattices measured using the CLE and reweighting as a function of the chemical potential.

## Acknowledgments

I would like to thank my collaborators G. Aarts, F. Attanasio, Z. Fodor, B. Jäger, S.D. Katz, E. Seiler, I.-O. Stamatescu, Cs. Török and the Gauss Centre for Supercomputing e.V. ([www.gauss-centre.eu](http://www.gauss-centre.eu)) for providing computing time on the GCS Supercomputer SuperMUC at Leibniz Supercomputing Centre (LRZ, [www.lrz.de](http://www.lrz.de)), as well as for providing computing time through the John von Neumann Institute for Computing (NIC) on the GCS share of the supercomputer JURECA and JUQUEEN [16] at Jülich Supercomputing Centre (JSC).

## References

- [1] P. de Forcrand, PoS LAT **2009**, 010 (2009) [arXiv:1005.0539]; G. Aarts, PoS LATTICE **2012** (2012) 017 [arXiv:1302.3028].
- [2] G. Parisi, Phys. Lett. **131 B** (1983) 393; J. Klauder, Acta Phys. Austr. Suppl. **XXXV** (1983) 251.
- [3] F. Pham, Proc. Symp. Pure Math. **40**, 319 (1983); E. Witten, arXiv:1001.2933; M. Cristoforetti, F. Di Renzo and L. Scorzato, Phys. Rev. D **86**, 074506 (2012), arXiv:1205.3996.
- [4] P. H. Damgaard and H. Hufel, Phys. Rept. **152** (1987) 227. doi:10.1016/0370-1573(87)90144-X
- [5] G. Aarts, E. Seiler and I. -O. Stamatescu, Phys. Rev. D **81** (2010) 054508 [arXiv:0912.3360]; G. Aarts, F. A. James, E. Seiler and I. -O. Stamatescu, Eur. Phys. J. C **71** (2011) 1756 [arXiv:1101.3270].
- [6] E. Seiler, D. Sexty and I. -O. Stamatescu, Phys. Lett. B **723**, 213 (2013) [arXiv:1211.3709 [hep-lat]]; G. Aarts, L. Bongiovanni, E. Seiler, D. Sexty and I. -O. Stamatescu, Eur. Phys. J. A **49** (2013) 89 doi:10.1140/epja/i2013-13089-4 [arXiv:1303.6425 [hep-lat]].
- [7] D. Sexty, Phys. Lett. B **729** (2014) 108 [arXiv:1307.7748 [hep-lat]].
- [8] G. Aarts, E. Seiler, D. Sexty and I. O. Stamatescu, Phys. Rev. D **90** (2014) 11, 114505; D. Sexty, PoS LATTICE **2014** (2014) 016 [arXiv:1410.8813 [hep-lat]].
- [9] A. Mollgaard and K. Splittorff, Phys. Rev. D **88** (2013) 116007 [arXiv:1309.4335 [hep-lat]]; J. Greensite, Phys. Rev. D **90** (2014) no.11, 114507 [arXiv:1406.4558 [hep-lat]].
- [10] G. Aarts, E. Seiler, D. Sexty, I.-O. Stamatescu, in prep.
- [11] K. Nagata, J. Nishimura and S. Shimasaki, arXiv:1604.07717 [hep-lat].
- [12] R. De Pietri, A. Feo, E. Seiler and I. O. Stamatescu, Phys. Rev. D **76** (2007) 114501 doi:10.1103/PhysRevD.76.114501 [arXiv:0705.3420 [hep-lat]].
- [13] G. Aarts, F. Attanasio, B. Jäger, E. Seiler, D. Sexty and I. O. Stamatescu, PoS LATTICE **2014** (2014) 200 [arXiv:1411.2632 [hep-lat]]; G. Aarts, F. Attanasio, B. Jäger, E. Seiler, D. Sexty and I.-O. Stamatescu, in prep.
- [14] Z. Fodor, S. D. Katz, D. Sexty and C. Török, Phys. Rev. D **92** (2015) no.9, 094516 doi:10.1103/PhysRevD.92.094516 [arXiv:1508.05260 [hep-lat]].
- [15] Z. Fodor and S. D. Katz, Phys. Lett. B **534** (2002) 87 doi:10.1016/S0370-2693(02)01583-6 [hep-lat/0104001].
- [16] Jülich Supercomputing Centre. (2015). JUQUEEN: IBM Blue Gene/Q Supercomputer System at the Jülich Supercomputing Centre. Journal of large-scale research facilities, 1, A1. <http://dx.doi.org/10.17815/jlsrf-1-18>